http://journal.uir.ac.id/index.php/JGEET

E-ISSN : 2541-5794
P-ISSN : 2503-216X

Journal of Geoscience,
Engineering, Environment, and Technology
Vol 10 No 1 2025

RESEARCH ARTICLE

Continuity Analysis of Groundwater Aquifers Using Geoelectrical Vertical Electrical Sounding (VES) Method with Schlumberger Configuration in Serayu-Citanduy Road and Golf Course, Tanah Merah Village, North Samarinda District, Indonesia

Hengky Himawan Sadewo [1,*], Djayus[1,2], Mislan[1], Piter Lepong[2]

[1] *Department of Physics, Mulawarman University, Samarinda, East Kalimantan, Indonesia.*
[2] *Department of Geophysics, Mulawarman University, Samarinda, East Kalimantan, Indonesia.*

* Corresponding author : himawan.hengky@gmail.com
Received: Sept 21, 2022; Accepted: Feb 10, 2025.
DOI: 10.25299/jgeet.2025.10.1.10571

Abstract

This study aims to analyze the continuity of the aquifer system between the Serayu-Citanduy area and the Golf Course area in Tanah Merah Village, North Samarinda District, using the Vertical Electrical Sounding (VES) method with Schlumberger configuration. Building on previous research that compared geoelectrical mapping and sounding methods for identifying aquifer layers in the Serayu-Citanduy area, this study focuses on aquifer connectivity based on resistivity profiles and geological interpretation. The VES data collected from eight measurement points revealed significant variations in lithology and aquifer types. At the Golf Course, the surface layer consists of soil (0.8 to 2.6 m depth), overlying a thick silt layer (up to 160 m depth) and a permeable sandstone aquifer between depths of 152.7 m and 160 m. The resistivity of the sandstone aquifer is approximately 20-50 Ωm. Meanwhile, at the Serayu-Citanduy Road, the lithology is divided into five main layers, with the surface layer (0.8 to 2.5 m) followed by a silt layer (5.2 to 22.9 m) and a sandstone layer from 22.9 m to 200 m depth. The resistivity of the sandstone aquifer here is higher, ranging from 50 to 150 Ωm, and is identified as an unconfined aquifer above a shale layer. Below 100.1 m, a confined aquifer is found beneath the shale layer, with resistivity values exceeding 100 Ωm. The correlation between the VES points at the Golf Course and Serayu-Citanduy Road shows continuity between the aquifer systems despite variations in thickness. These findings provide new insights into the hydrogeology of Tanah Merah and highlight the importance of groundwater management strategies for sustainable water use in North Samarinda District.

Keywords: Aquifer Continuity, Vertical Electrical Sounding (VES), Schlumberger Configuration, Groundwater, Resistivity Profiles

1. Introduction

Water plays an important role as a basic need for the development of human welfare and plays a role in human survival (Hadian et al., 2017). Groundwater is one of the most important resources that supports human life and various economic activities, particularly in areas with limited surface water resources. According to (Fetter, 2001), groundwater is stored in the saturated zones of soils and rocks, moving through pores or fractures as groundwater flow, and eventually filling bodies of water such as lakes, rivers, and seas. As domestic, agricultural, and industrial needs increase, excessive exploitation of aquifers can lead to a decline in the groundwater table, which affects the availability and quality of these water resources (Rezky et al., 2019; Juandi, 2019).

Tanah Merah Village, North Samarinda District, is one of the areas that relies on groundwater as the primary source to meet daily needs. The challenging topography and lack of clean water distribution infrastructure are the main reasons for this reliance. In this context, geophysical methods such as Geoelectrical Vertical Electrical Sounding (VES) with the Schlumberger configuration have been used to map aquifer layers and assess groundwater potential (Darisma et al., 2020; Bahri et al., 2023). This method is highly effective in identifying rock layers with low resistivity values, which indicate the presence of aquifers (Telford et al., 1990).

Previous studies have shown that the aquifer layers in the Serayu-Citanduy area have significant potential, with semi-confined aquifer layers found at certain depths. However, studies on the continuity and hydrogeological relationships of aquifers between this area and surrounding areas, such as the Golf Course area, are still limited (Djayus et al., 2017). Understanding aquifer continuity is crucial for sustainable groundwater resource management to prevent overexploitation and contamination (Bahri et al., 2023).

Studies in other regions, such as research in Leihitu, Maluku, and Kemuning, Riau, highlight the importance of analyzing hydrogeological parameters such as longitudinal conductance and transverse resistance to assess the protective capacity and transmissivity of aquifers (Bahri et al., 2023; Juandi et al., 2020). These parameters provide important information on the aquifer's ability to store and distribute water, as well as its resistance to surface contamination or seawater intrusion. Using geophysical approaches, parameters such as storativity and hydraulic conductivity can also be integrated into models to predict long-term groundwater availability (Juandi, 2020).

This research is a continuation of previous studies conducted by the author, which focused on comparing geoelectric mapping and sounding methods to identify aquifer layers in the Serayu-Citanduy area (Sadewo et al., 2024). Based on these findings, this study aims to analyze the continuity of the aquifer system between the Serayu-Citanduy area and the Golf Course area, providing new insights into integrated hydrogeology in Tanah Merah Village. By using the Vertical Electrical Sounding (VES) method with the Schlumberger configuration, this study evaluates aquifer connectivity based on resistivity profiles and geological interpretation.

Through the examination of the hydrogeological relationship between these two regions, this study contributes to a deeper understanding of the potential groundwater resources in Tanah Merah. The findings from this research aim to support sustainable water management strategies and ensure long-term water security in North Samarinda District.

2. Research Area Setting and Geology

This study was conducted in Tanah Merah Village, North Samarinda District, with a focus on two distinct areas: the Serayu-Citanduy Road and the Golf Course. These locations were chosen for their contrasting topographical and geological characteristics, providing an opportunity to study aquifer connectivity across varied terrains. A total of eight Vertical Electrical Sounding (VES) points were surveyed, with five located along Serayu-Citanduy Road and three in the Golf Course area. The measurements employed the Schlumberger configuration, which is well-suited for subsurface investigations due to its ability to probe deeper layers as the current electrode spacing increases. Current was injected through the outer electrodes, while the inner electrodes measured the potential difference, enabling resistivity analysis of subsurface layers (Sadewo et al., 2024).

The Serayu-Citanduy Road section primarily features lowland topography, with elevations starting at 3.07 meters above sea level, as derived from Digital Elevation Model National (DEMNAS) data (Sadewo et al., 2024). The geological composition in this area is part of the Balikpapan Formation, consisting of sandstone, claystone, silt, shale, limestone, and occasional coal seams (Supriatna et al., 1995). Outcrop observations confirmed the presence of quartz sandstone with a yellowish-white hue, a characteristic feature of this formation. These attributes provide a strong foundation for aquifer analysis in this region

In contrast, the Golf Course area is characterized by hilly terrain, with elevations reaching up to 81.3 meters. This topographical variation introduces unique subsurface conditions that influence aquifer behavior. Field measurements in this area identified similar lithological compositions to those found in the Serayu-Citanduy section, but with notable differences in elevation and potential aquifer connectivity. The inclusion of this area allows for a more comprehensive evaluation of the hydrogeological system in Tanah Merah, particularly in understanding the continuity of sandstone aquifers across varying geological settings.

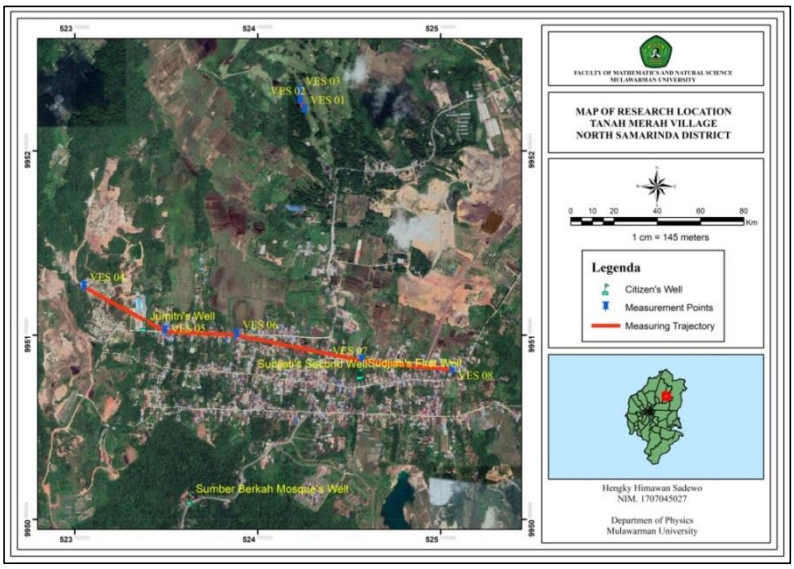

Fig. 1. Geoelectrical Measurement Location Map.

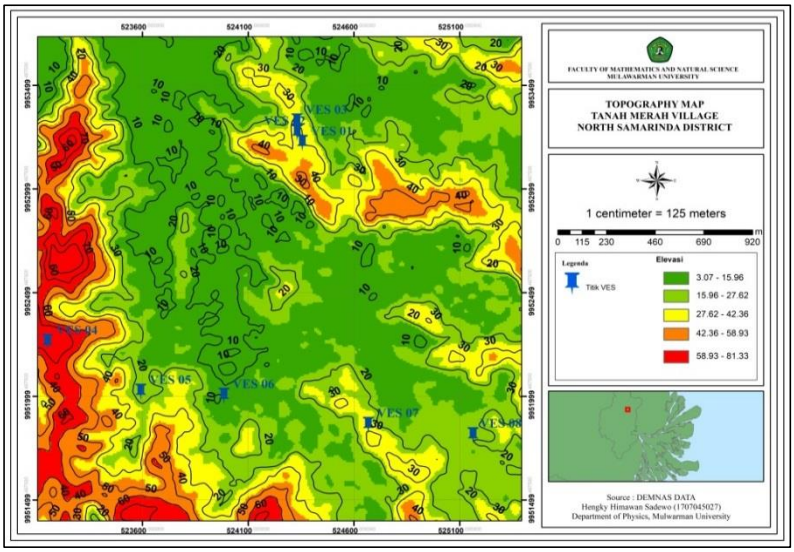

Fig. 2. Topographic Map of Research Area.

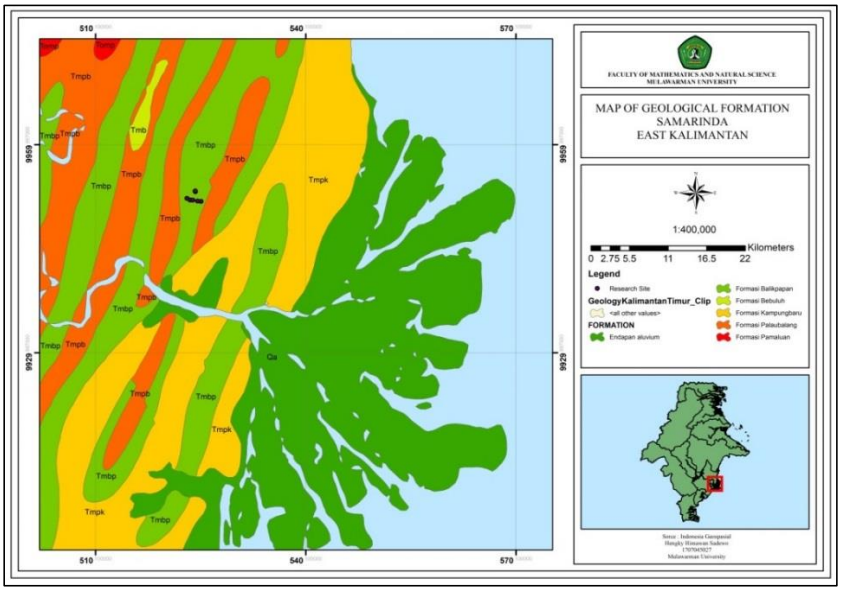

Fig. 3. Geological Map of Research Area.

3. Method

3.1 Geoelectrical Approach

This study uses the geoelectrical method to measure the resistivity of rock layers, which is influenced by various factors such as material type, density, porosity, water content, water quality, and temperature (Djayus et al., 2017). Lower resistivity often indicates the presence of an aquifer, which may consist of loose materials containing groundwater or salts (Telford et al., 1990). The basic concept of the geoelectrical method refers to Ohm's Law, first formulated by the German scientist George Simon Ohm (1787-1854). According to Ohm's Law, the potential difference (V) at the ends of a medium is directly proportional to the electric current (I) flowing through the medium (Pratama et al., 2019). Ohm's Law also states that electrical resistance (R) is directly proportional to the length of the medium (L) and inversely proportional to its cross-sectional area (A). The formulation of these two statements is

$$V = IR \quad (1)$$

$$R = \rho \frac{L}{A} \quad (2)$$

With V representing the potential difference (Volts), I the current (Amperes), R the electrical resistance (Ω), ρ the resistivity (Ω/m), L the length of the medium (m), and A the cross-sectional area (m²). The direction of the electric current is measured from the positive charge to the negative charge, although the convention states the opposite (Syukri, 2020). The use of this method is relevant for groundwater resource research due to its sensitivity to resistivity variations (Rezky et al., 2019).

According to (Menke, 2012) based on geoelectrical measurement techniques, there are two measurement techniques, namely the geoelectrical resistivity mapping method and sounding. Geoelectrical mapping for mapping the horizontal distribution of resistivity (Syifaurrohman et al., 2018), and sounding, which involves subsurface measurements to determine the vertical geoelectrical distribution up to a certain depth. This term originates from Vertical Electrical Sounding (VES), assuming no lateral effects in the direction of electrode spread (Suryo et al., 2016). In this study, the Vertical Electrical Sounding (VES) approach was chosen due to its ability to identify groundwater-bearing layers in detail (Bahri et al., 2023).

3.2 Schlumberger Configuration

The Schlumberger configuration uses four electrodes, with two potential electrodes and two current electrodes arranged in a straight line, where the distance between the potential electrodes is smaller than the distance between the current electrodes, as shown in Figure 4 (Usman et al., 2017). The electrode distance is proportional to the depth of the detected rock layers. The larger the electrode distance, the deeper the rock layers that can be detected. In field measurements, the electrode distance can be increased if using an adequate geoelectrical instrument. In this case, the instrument must be capable of generating a large current or a current sensitive enough to detect small potential differences in the earth (Febriana et al., 2017).

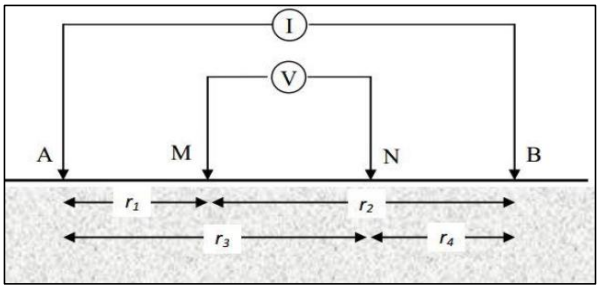

Fig. 4. Form of Electrode Configuration Schlumberger Method (Febriana et al., 2017).

With a is the distance between the electrodes M and N. Based on (figure 4) above, it is known that M,N = a and A,M = N,B = na , so $r_2 = r_3 = na + a$ and $r_1 = r_4 = na$. The results of these measurements can be used to calculate the magnitude of apparent-resistivity (ρ_a) Schlumberger configuration according to the following equation

$$\rho_a = 2\pi \left[\left\{\frac{1}{na} - \frac{1}{na+a}\right\} - \left\{\frac{1}{na+a} - \frac{1}{na}\right\}\right]^{-1} \frac{\Delta V}{I} \quad (1)$$

$$\rho_a = 2\pi \left[\frac{1}{na} - \frac{1}{na+a} - \frac{1}{na+a} + \frac{1}{na}\right]^{-1} \frac{\Delta V}{I} \quad (2)$$

$$\rho_a = 2\pi \left[\frac{2}{na} - \frac{2}{na+a}\right]^{-1} \frac{\Delta V}{I} \quad (3)$$

$$\rho_a = 2\pi \left[\frac{2(na+a)-2na}{na(na+a)}\right]^{-1} \frac{\Delta V}{I} \quad (4)$$

$$\rho_a = 2\pi \left[\frac{2a}{na(na+a)}\right]^{-1} \frac{\Delta V}{I} \quad (5)$$

$$\rho_a = 2\pi \left[\frac{na(na+a)}{2a}\right]\frac{\Delta V}{I} \quad (6)$$

$$\rho_a = \pi[n(na+a)]\frac{\Delta V}{I} \quad (7)$$

$$\rho_{as} = K_s \frac{\Delta V}{I} \quad (8)$$

(Hayon, 2017).

3.3 Research Stages

3.3.1 Preparation

This stage includes the collection of secondary data, such as the regional geological map of Samarinda and well data from local residents. The software IP2WIN, RockWork 16, and Microsoft Excel are used for processing the resistivity data.

3.3.2 Preliminary Survey

The preliminary survey aims to identify the initial conditions of the study location, including the observation of rock formations, morphology, and lithology through rock outcrops. This analysis facilitates the interpretation of field data (Usman et al., 2017).

3.3.3 Data Collection

Data collection is systematically conducted at eight measurement points: five along the Serayu-Citanduy Road and three at the Golf Course. The data acquisition process involves injecting current into the ground through current electrodes, while voltage values are recorded through potential electrodes (Ikhsan et al., 2018). Each sounding point is selected based on the geological map and a preliminary survey. The electrode spacing is set with a maximum length of 300 meters for the current electrodes (AB) and 40 meters for the potential electrodes (MN). Once the electrodes are positioned, the cables are connected to the measuring device. To ensure proper function of the equipment, an electrode connectivity test is performed before resistivity measurements are taken using the Schlumberger configuration (Rezky et al., 2019).

3.3.4 Data Processing

The resistivity data is processed using IP2WIN to generate an inversion model of the subsurface. The software RockWork 16 is used to create 2D contours that connect the results from all sounding points (Hayon, 2017).

3.3.5 Analysis and Interpretation

The processed data is analyzed to determine the lithology type based on its resistivity values. Layers considered to be aquifers are identified and compared with well data from local residents for further validation. This data provides insight into the continuity of the aquifer system in the study area (Maay et al., 2022).

4. Result and Interpretation

4.1. Result and Interpretation

The morphology of the study area, based on the National Digital Elevation Model (DEMNAS) data, has an elevation ranging from 3.07 to 81.3 meters above sea level, as shown in Figure 2. The study area is dominated by hills and lowlands. Additionally, based on field outcrop observations, the geological investigation shows that the outcrop on Serayu Road has a dip of 46° to the east, and the outcrop on Citanduy Road has a dip of 30° to the west, as shown in Figure 5.

Next, well depth data from local residents was collected to verify the depth of the groundwater table below the surface and to facilitate interpretation. The collected data includes well depth and well characteristics during the dry season. This aims to identify aquifer characteristics and the potential groundwater content within it. The well data from local residents is presented in Table 1.

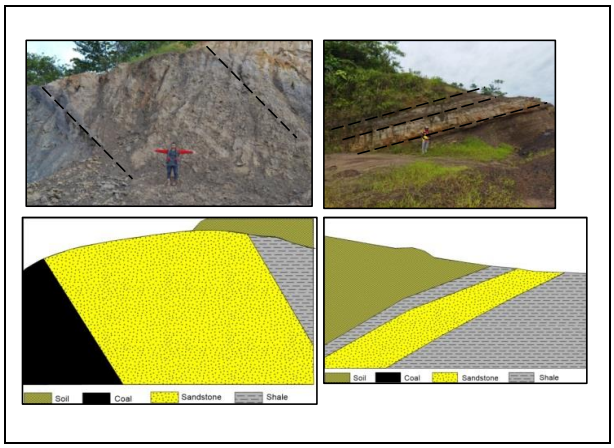

Fig. 5. Outcrops on Serayu and Citanduy Roads

Table 1. Well Data from Local Residents

Well	Coordinate		Depth	Description
	X	Y		
Ibu Jumitri	-0.4338	117.211	20	Never runs dry, and the water quality is clear
Ibu Sudjiati 1	-0.4361	117.222	18	Never runs dry, and the water quality is clear, has received certification and is sold
Ibu Sudjiati 2	-0.4362	117.222	12	
Mushola Subur Berkah	-0.4423	117.213	125	Never runs dry, and the water quality is clear

4.2 Results of VES Processing at Golf Course

4.2.1 VES Point 01

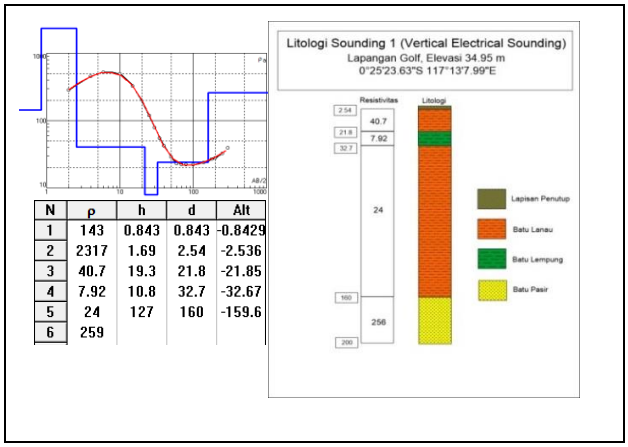

N	ρ	h	d	Alt
1	143	0.843	0.843	-0.8429
2	2317	1.69	2.54	-2.536
3	40.7	19.3	21.8	-21.85
4	7.92	10.8	32.7	-32.67
5	24	127	160	-159.6
6	259			

Fig 6. Results of VES 1 Processing

Based on the processing results, VES Point 1, as shown in Figure 6, is identified as consisting of 6 layers. The first layer has a resistivity of 143 Ωm at a depth of 0.84 m from the surface, the second layer has a resistivity of 2317 Ωm at a depth of 2.54 m from the surface, interpreted as soil (cover layer). The third layer has a resistivity of 40.7 Ωm at a depth of 21.8 m from the surface, interpreted as silt. The fourth layer has a resistivity of 7.92 Ωm at a depth of 32.7 m from the surface, interpreted as clay. The fifth layer has a resistivity of 24 Ωm at a depth of 160 m from the surface, interpreted as silt, and the last layer has a resistivity of 259 Ωm at a depth below 160 m from the surface, interpreted as sandstone.

4.2.2 VES Point 02

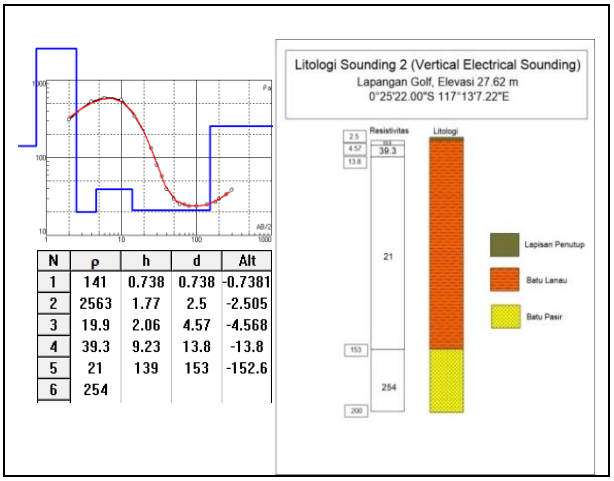

N	ρ	h	d	Alt
1	141	0.738	0.738	-0.7381
2	2563	1.77	2.5	-2.505
3	19.9	2.06	4.57	-4.568
4	39.3	9.23	13.8	-13.8
5	21	139	153	-152.6
6	254			

Fig 7. Results of VES 2 Processing

Based on the processing results, VES Point 2, as shown in Figure 7, is identified as consisting of 6 layers. The first layer has a resistivity of 141 Ωm at a depth of 0.738 m from the surface, the second layer has a resistivity of 2563 Ωm at a depth of 2.5 m from the surface, the third layer has a resistivity of 19.9 Ωm at a depth of 4.57 m from the surface, interpreted as soil (cover layer). The fourth layer has a resistivity of 39.3 Ωm at a depth of 9.23 m from the surface, interpreted as silt. The fifth layer has a resistivity of 21 Ωm at a depth of 153 m from the surface, interpreted as silt, and the last layer has a resistivity of 254 Ωm at a depth below 153 m from the surface, interpreted as sandstone.

4.2.3 VES Point 03

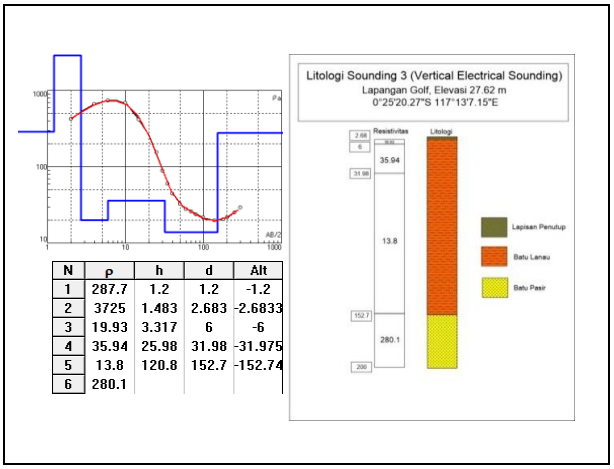

N	ρ	h	d	Alt
1	287.7	1.2	1.2	-1.2
2	3725	1.483	2.683	-2.6833
3	19.93	3.317	6	-6
4	35.94	25.98	31.98	-31.975
5	13.8	120.8	152.7	-152.74
6	280.1			

Fig 8. Results of VES 3 Processing

Based on the processing results, VES Point 3, as shown in Figure 8, is identified as consisting of 6 layers. The first layer has a resistivity of 287.7 Ωm at a depth of 1.2 m from the surface, the second layer has a resistivity of 3725 Ωm at a depth of 2.683 m from the surface, the third layer has a resistivity of 19.93 Ωm at a depth of 6 m from the surface, interpreted as soil (cover layer). The fourth layer has a resistivity of 35.94 Ωm at a depth of 31.98 m from the surface, interpreted as silt. The fifth layer has a resistivity of 13.8 Ωm at a depth of 152.7 m from the surface, interpreted as silt, and the last layer has a resistivity of 280.1 Ωm at a depth below 152.7 m from the surface, interpreted as sandstone.

4.3 Results of VES Processing at Serayu-Citanduy

4.3.1 VES Point 04

Based on the VES 4 processing results, as shown in Figure 9, it is identified as consisting of 6 layers. The first layer has a resistivity of 112.4 Ωm at a depth of 2.508 m from the surface, the second layer has a resistivity of 35.96 Ωm at a depth of 5.242 m from the surface, the third layer has a resistivity of 212.5 Ωm at a depth of 10.95 m from the surface, interpreted as soil (cover layer). The fourth layer has a resistivity of 275.9 Ωm at a depth of 22.89 m from the surface, interpreted as sandstone. The fifth layer has a resistivity of 839 Ωm at a depth of 100.1 m from the surface, interpreted as shale, and the last layer has a resistivity of 180.1 Ωm at a depth below 100.1 m from the surface, interpreted as sandstone.

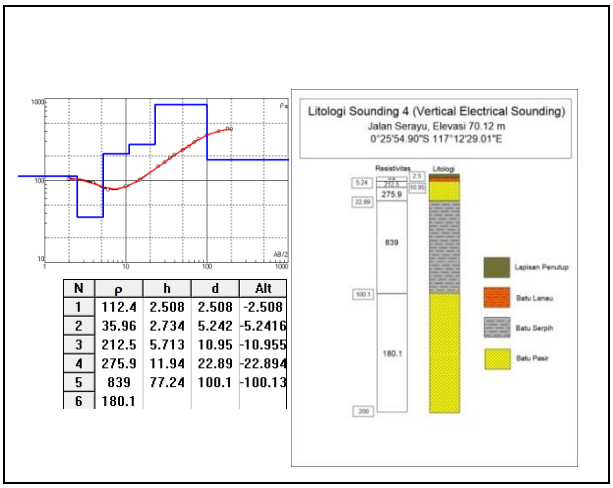

N	ρ	h	d	Alt
1	112.4	2.508	2.508	-2.508
2	35.96	2.734	5.242	-5.2416
3	212.5	5.713	10.95	-10.955
4	275.9	11.94	22.89	-22.894
5	839	77.24	100.1	-100.13
6	180.1			

Fig 9. Results of VES 4 Processing

4.3.2 VES Point 05

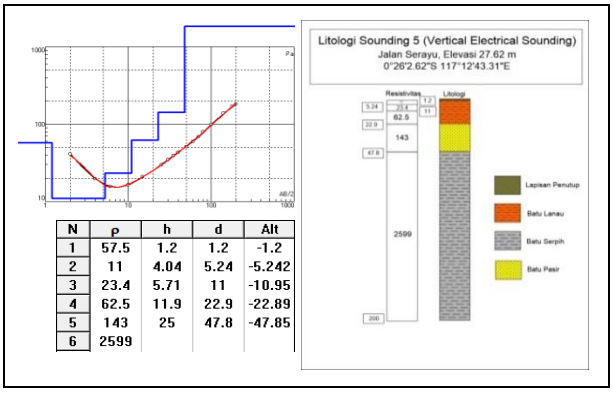

N	ρ	h	d	Alt
1	57.5	1.2	1.2	-1.2
2	11	4.04	5.24	-5.242
3	23.4	5.71	11	-10.95
4	62.5	11.9	22.9	-22.89
5	143	25	47.8	-47.85
6	2599			

Fig 10. Results of VES 5 Processing

Based on the processing results, VES 5, as shown in Figure 10, is identified as consisting of 6 layers. The first layer has a resistivity of 57.5 Ωm at a depth of 1.2 m from the surface, the second layer has a resistivity of 11 Ωm at a depth of 5.24 m from the surface, the third layer has a resistivity of 23.4 Ωm at a depth of 11 m from the surface, interpreted as soil (cover layer). The fourth layer has a resistivity of 62.5 Ωm at a depth of 22.9 m from the surface, interpreted as silt. The fifth layer has a resistivity of 143 Ωm at a depth of 47.8 m from the surface, interpreted as sandstone, and the last layer has a resistivity of 2599 Ωm at a depth below 47.8 m from the surface, interpreted as shale.

4.3.3 VES Point 06

Based on the processing results, as shown in Figure 11, VES 6 is identified as consisting of 6 layers. The first layer has a resistivity of 76.9 Ωm at a depth of 1.2 m from the surface, the second layer has a resistivity of 10.1 Ωm at a depth of 2.51 m from the surface, the third layer has a

resistivity of 112 Ωm at a depth of 5.24 m from the surface, the fourth layer has a resistivity of 20.1 Ωm at a depth of 11 m from the surface, interpreted as soil (cover layer). The fifth layer has a resistivity of 217 Ωm at a depth of 49.5 m from the surface, interpreted as sandstone, and the last layer has a resistivity of 131 Ωm at a depth below 49.5 m from the surface, interpreted as sandstone.

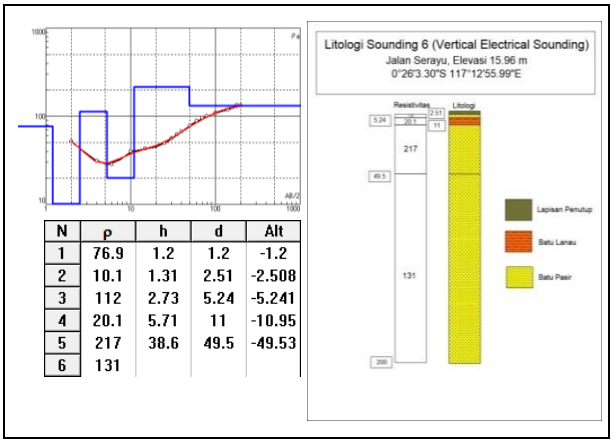

N	ρ	h	d	Alt
1	76.9	1.2	1.2	-1.2
2	10.1	1.31	2.51	-2.508
3	112	2.73	5.24	-5.241
4	20.1	5.71	11	-10.95
5	217	38.6	49.5	-49.53
6	131			

Fig 11. Results of VES 6 Processing

4.3.4 VES Point 07

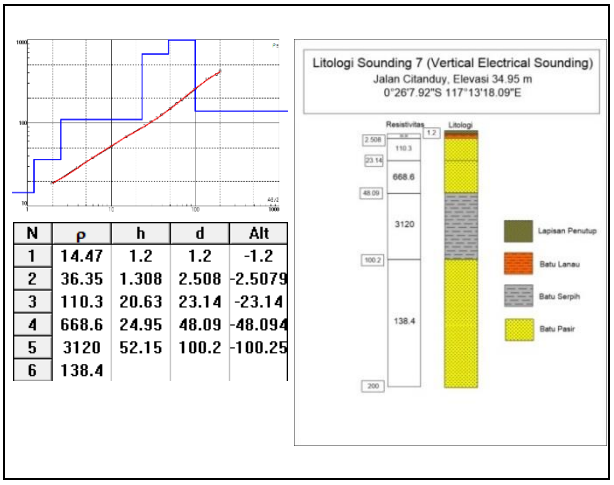

N	ρ	h	d	Alt
1	14.47	1.2	1.2	-1.2
2	36.35	1.308	2.508	-2.5079
3	110.3	20.63	23.14	-23.14
4	668.6	24.95	48.09	-48.094
5	3120	52.15	100.2	-100.25
6	138.4			

Fig 12. Results of VES 7 Processing

Based on the curve above, the processing result of VES 7, as shown in Figure 12, is identified as consisting of 6 layers. The first layer has a resistivity of 14.47 Ωm at a depth of 1.2 m from the surface, the second layer has a resistivity of 36.35 Ωm at a depth of 2.508 m from the surface, interpreted as soil (cover layer). The third layer has a resistivity of 110.3 Ωm at a depth of 23.14 m from the surface, interpreted as sandstone. The fourth layer has a resistivity of 668.6 Ωm at a depth of 48.09 m from the surface, interpreted as sandstone. The fifth layer has a resistivity of 3120 Ωm at a depth of 100.2 m from the surface, interpreted as shale, and the last layer has a resistivity of 138.4 Ωm at a depth below 100.2 m from the surface, interpreted as sandstone.

4.3.5 VES Point 08

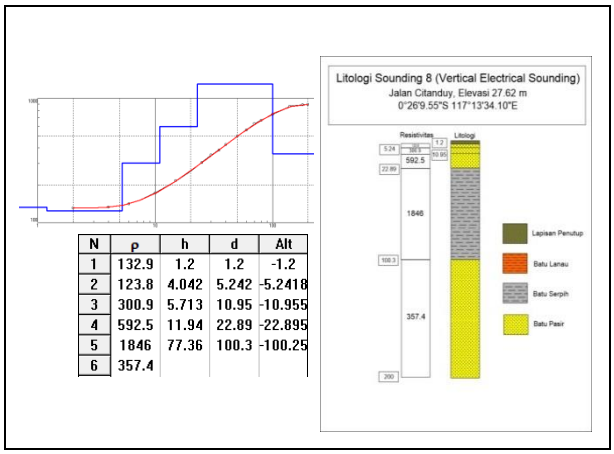

N	ρ	h	d	Alt
1	132.9	1.2	1.2	-1.2
2	123.8	4.042	5.242	-5.2418
3	300.9	5.713	10.95	-10.955
4	592.5	11.94	22.89	-22.895
5	1846	77.36	100.3	-100.25
6	357.4			

Fig 13. Results of VES 8 Processing

Based on the processing results, VES 8, as shown in Figure 13, is identified as consisting of 6 layers. The first layer has a resistivity of 132.9 Ωm at a depth of 1.2 m from the surface, interpreted as soil (cover layer). The second layer has a resistivity of 123.8 Ωm at a depth of 5.242 m from the surface, interpreted as sandstone. The third layer has a resistivity of 300.9 Ωm at a depth of 10.95 m from the surface, interpreted as sandstone. The fourth layer has a resistivity of 592.5 Ωm at a depth of 22.89 m from the surface, interpreted as sandstone. The fifth layer has a resistivity of 1846 Ωm at a depth of 100.3 m from the surface, interpreted as shale, and the last layer has a resistivity of 357.4 Ωm at a depth below 100.3 m from the surface, interpreted as sandstone.

5. Discussion

5.1 VES Inversion Results at Golf Course

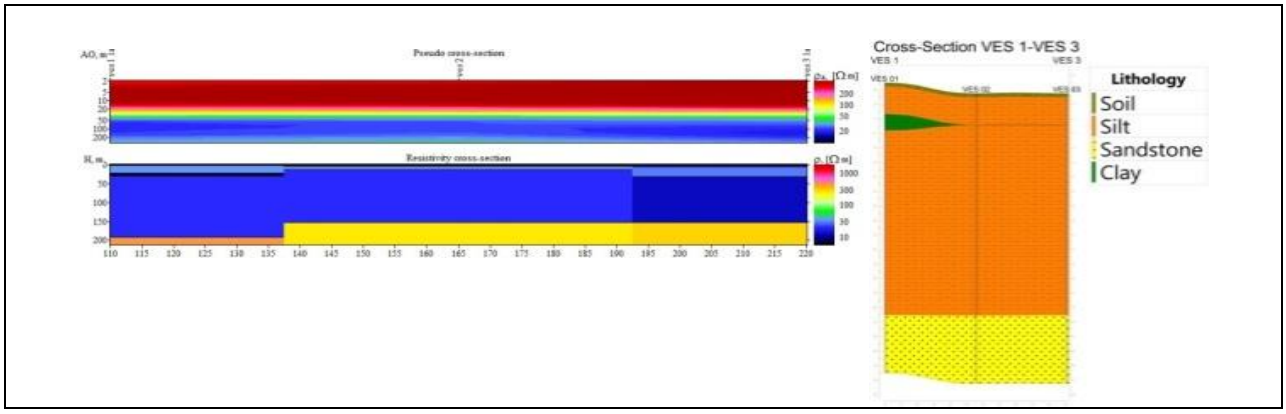

Fig 14. Golf Course Lithology Section

Based on the cross-section at the first location shown in Figure 14, the highest elevation is found at VES 1, which is 34.95 meters above sea level, while the lowest elevation is at VES 2 and VES 3, which is 27.62 meters above sea level. The lithology in this section is divided into three main layers. The first layer is the surface layer, identified as soil, with a depth

ranging from 0.8 meters to 2.6 meters. The second layer is silt, extending down to 160 meters. Within this layer, a clay intercalation was found at a depth of 21.8 meters from the surface. The final layer is sandstone, located beneath a depth of 160 meters. The aquifer in this section is marked by a permeable sandstone layer, located between depths of 152.7 meters to 160 meters. The type of aquifer at this location is identified as a leaky aquifer, as it is situated beneath a silt layer, which is aquiclude in nature.

5.2 VES Inversion Results at Serayu-Citanduy

Based on the cross-section at the second location shown in Figure 15, the highest elevation is found at VES 4, which is 70.12 meters above sea level, while the lowest elevation is at VES 6, which is 15.96 meters above sea level. The lithology in this section is divided into five main layers. The first layer is the surface layer, identified as soil, with a depth ranging from 1.2 meters to 2.5 meters. The second layer is silt, with a depth of 5.2 to 22.9 meters. The third layer is sandstone, starting at a depth of 22.9 meters and forming a basin down to 200 meters. The fourth layer is shale, with a depth ranging from 100.1 meters to 200 meters, and the final layer is sandstone, located below a depth of 100.1 meters. The aquifer in this section is marked by a permeable sandstone layer at depths ranging from 5.24 meters to 200 meters and below 100.1 meters. The first aquifer, located above the shale layer, is identified as an unconfined aquifer because there is no confining layer above it. This aquifer forms a basin, referred to as the Groundwater Basin. The second aquifer, located below the shale layer, is identified as a confined aquifer because it is located beneath the shale layer, which is aquiclude in nature.

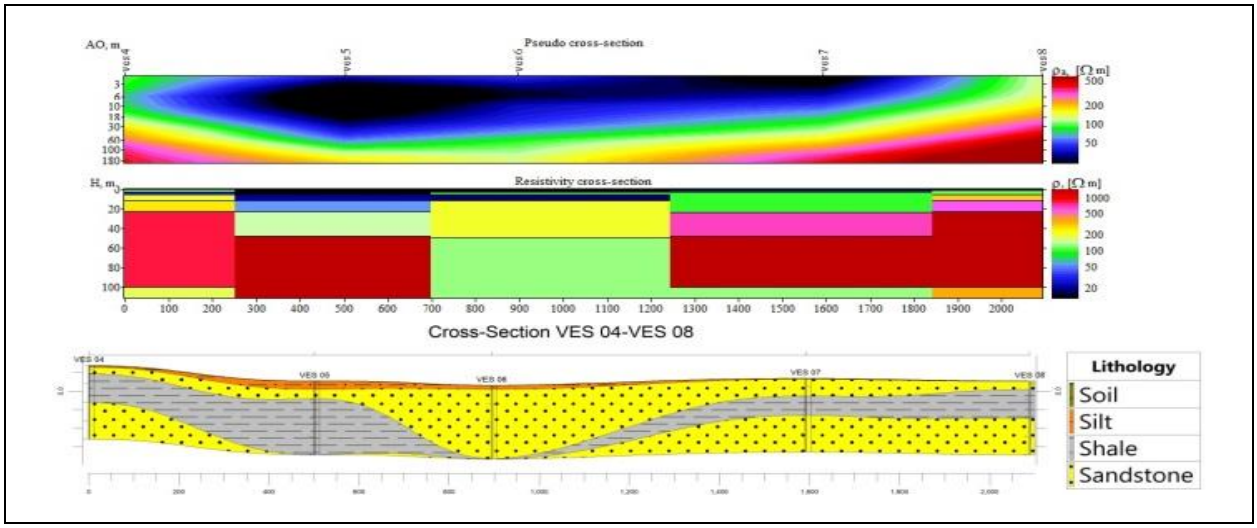

Fig 15. Serayu-Citanduy Road Lithology Section

5.3 Continuity of Aquifer Layers at Golf Course and Serayu-Citanduy

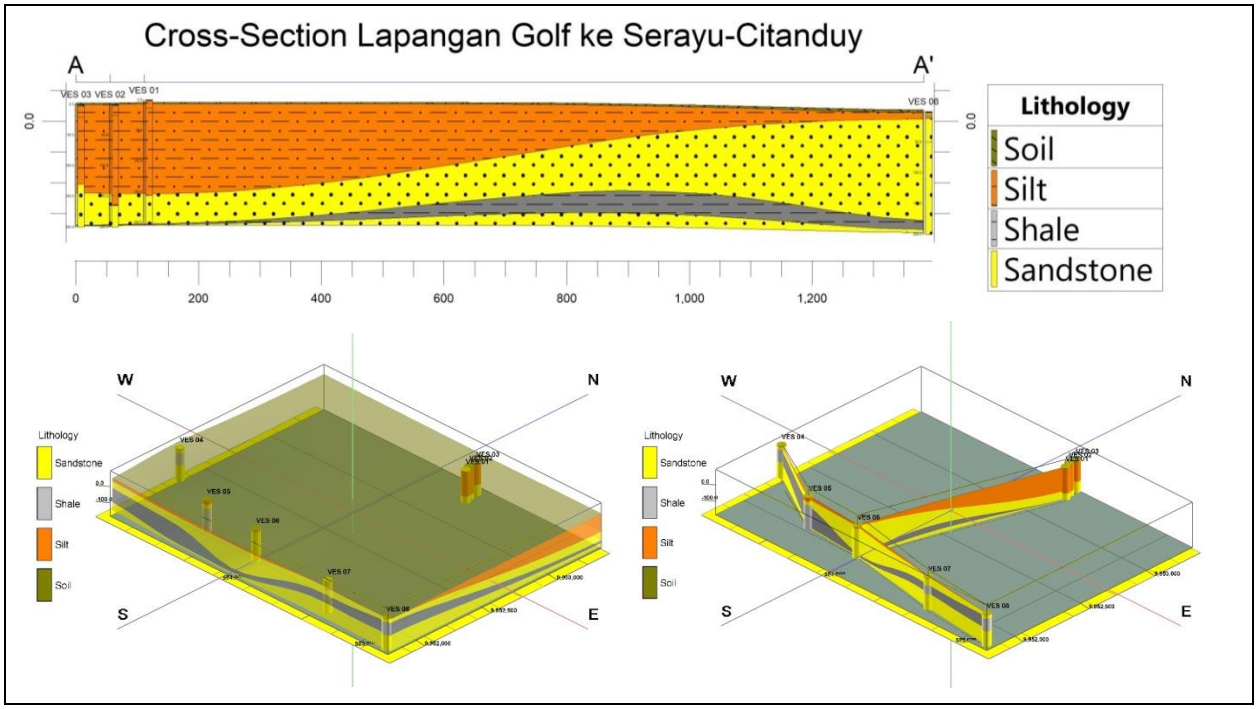

Fig 16. Cross Section between Golf Course and Serayu-Citanduy

Based on the cross-section in Figure 16, there is a correlation between the VES points at the Golf Course and Serayu-Citanduy Road. At the Golf Course, the silt layer is relatively thick, extending to a depth of 160 meters. However,

as one moves south toward Serayu-Citanduy, this layer thins out, reaching a maximum depth of only 22.9 meters. A decrease in elevation is also observed, from 27.62 meters at VES 3 (Golf Course) to 15.96 meters at VES 6 (Serayu-Citanduy), although the change is not significant. Consequently, the underlying sandstone layer becomes thicker toward the south, from a depth of 160 meters at the Golf Course to 22.9 meters to 200 meters at Serayu-Citanduy Road. This sandstone layer is identified as an aquifer. The cross-section shows that, despite variations in thickness and thinning, the lithology layers remain connected to each other.

The type of aquifer at the Golf Course is identified as a leaky aquifer which is characterized by a layer of sandstone at a depth of 152.7-160 m below the silt layer. This silt layer is a continuation of the silt layer on the Serayu-Citanduy Road section. However, the layer of silt on the Serayu-Citanduy road section is in the water table zone, so the aquifer identified at this location is an unconfined aquifer because there is no confinement layer at the top. This free aquifer forms a basin from a depth of 5.24 meters to a depth of 200 meters. Subsequently, the Confined Aquifer was identified at a depth of below 100.1 meters under the shale layer. Shale at this location, identified as an aquifer which is the dividing line between the unconfined aquifer and the confined aquifer.

The existence of an aquifer at the study site was confirmed by citizen's well with a depth of between 12 and 125 meters. The unconfined aquifer on the Serayu Street section has a depth that corresponds to the well of Ma'am Jumitri at a depth of 20 m, while those on Citanduy Street have the same depth as the well of Ma'am Sudjiati at a depth of 12 – 18 m. Furthermore, the syncline lower arc which is further identified as the lower arc of the Groundwater Basin, its existence is confirmed by the well of the Sumber Berkah Mosque with a depth of 125 m.

6. Conclusion

Based on the analysis and inversion results of the VES data from the Golf Course and Serayu-Citanduy Road, variations in lithology and aquifer types between the two locations were observed. At the Golf Course, the silt layer is thick, extending to a depth of 160 meters, underlain by a sandstone layer forming a leaky aquifer. This unconfined aquifer creates a groundwater basin due to the absence of an overlying confining layer. Conversely, at Serayu-Citanduy Road, the silt layer thins toward the south, with the sandstone layer becoming thicker. Here, a confined aquifer forms beneath a shale layer that acts as an aquiclude, restricting vertical water movement. The change in elevation from the Golf Course to Serayu-Citanduy Road influences the thickness and extent of the aquifer layers, with thicker aquifer formations observed toward the south.

This study demonstrates the hydrogeological continuity of interconnected aquifer layers across the two locations, despite variations in lithological thickness. The groundwater basin at the Golf Course offers significant storage potential, while the confined aquifer at Serayu-Citanduy Road represents a crucial resource for groundwater extraction. These findings underscore the importance of carefully monitoring and managing these aquifers to sustain water availability in the region.

Furthermore, this study highlights the critical role of understanding aquifer continuity for sustainable groundwater resource management. The identification of interconnected aquifers between Serayu-Citanduy Road and the Golf Course supports the development of integrated water management strategies in Tanah Merah Village. By distributing groundwater extraction evenly across these aquifers, the risks of over-extraction and resource depletion can be minimized. Additionally, these findings provide a foundation for future hydrogeological studies and infrastructure development in North Samarinda District.

Acknowledgment

The authors would like to express their gratitude to the Department of Physics, Faculty of Mathematics and Natural Sciences, Mulawarman University, for providing the facilities and support necessary to conduct this research. Special thanks are extended to Dr. Eng. Idris Mandang, M.Si., for his invaluable guidance and constructive feedback throughout the research and manuscript preparation process.

References

Bahri, S., Ramadhan, A., & Zulfiah. (2023). Investigation of Groundwater Quality using Vertical Electrical Sounding and Dar Zarrouk Parameter in Leihitu, Maluku, Indonesia. Journal of Geoscience, Engineering, Environment, and Technology, 8(3), 221–228. https://doi.org/10.25299/jgeet.2023.8.3.12976.

Darisma, D., Fernanda, F., & Syukri, M. (2020). Investigation of Groundwater Potential using Electrical Resistivity Method and Hydraulic Parameters in Lam Apeng, Aceh Besar, Indonesia. Journal of Geoscience, Engineering, Environment, and Technology, 5(4), 185–192. https://doi.org/10.25299/jgeet.2020.5.4.5501.

Djayus, Hardwinarto, S., Subagiyo, L., & Sumaryono. (2017). Study Of Land Cover And Condition Catchment Area Groundwater Aquifer In Tanah Merah North Samarinda District Using Resistivity Geoelectric Sounding. International Journal of Scientific & Technology Research, 6(6), 126–128.

Febriana, R. K. N., Minarto, E., & Tryono, F. Y. (2017). Identifikasi Sebaran Aliran Air Bawah Tanah (Groundwater) dengan Metode Vertical Electrical Sounding (VES) Konfigurasi Schlumberger di Wilayah Cepu, Blora Jawa Tengah. Jurnal Sains Dan Seni ITS, 6(2), 6–10. https://doi.org/10.12962/j23373520.v6i2.25280.

Fetter, C. W. (2001). Applied Hydrogeology (4th ed.). Prentice Hall.

Hadian, M. S. D., Waliana, T. Y., Sulaksana, N., Putra, D. B. E., & Yuskar, Y. (2017). Hydrochemistry and Characteristics of Groundwater: Case Study Water Contamination at Citarum River Upstream. Journal of Geoscience, Engineering, Environment, and Technology, 2(4), 268. https://doi.org/10.24273/jgeet.2017.2.4.578

Hayon, Marianus Aneng. (2017). Perbandingan Metode Geolistrik Konfigurasi Wenner-Schlumberger dan Dipole-Dipole Dengan Data Bore Hole Untuk Identifikasi Longsor Di Areal Jalan Ringroud Kelurahan Lok Bahu Kecamatan Sungai Kunjang Samarinda. Skripsi Sarjana Sains. Program Studi Fisika FMIPA, Universitas Mulawarman.

Ikhsan, M., Farid, F., Samsidar, & Handayani, L. (2018). Penentuan struktur tanah sebagai dasar uji kelayakan kekuatan bangunan perumahan di Muaro Jambi menggunakan metode geolistrik konfigurasi dipole-dipole. Komunikasi Fisika Indonesia, 15(2). https://doi.org/10.1234/komfisika.2018.15202

Juandi, M. (2020). Water sustainability model for estimation of groundwater availability in Kemuning District, Riau-Indonesia. Journal of Groundwater Science and Engineering, 8(1), 20–29. https://doi.org/10.19637/j.cnki.2305-7068.2020.01.003.

Maay, B. R., & Supit, J. M. (2022). Interpretasi dan korelasi data resistivitas untuk menentukan lapisan akuifer di

RT.002/RW.002 Kelurahan Amban Kabupaten Manokwari Provinsi Papua Barat. INTAN Jurnal Penelitian Tambang, 4(2), 93. https://doi.org/10.56139/intan.v4i2.89

Menke, W. (2012). Geophysical Data Analysis Discrete Inverse Theory, Third Edition MATLAB Edition. In Geophysical Data Analysis: Discrete Inverse Theory. https://doi.org/10.1016/b978-0-12-397160-9.00001-1

Pratama, I. E., Muhtar, I. J., Syamsuddin, & Aswad, S. (2019). Identifikasi batuan dasar daerah Pantai Lumpue Kota Parepare menggunakan metode geolistrik konfigurasi Wenner. Jurnal Geocelebes, 3(1), 47-50. https://doi.org/10.20956/geocelebes.v3i1.6397

Rezky, B., Mandang, I., & Lepong, P. (2019). Identification of Groundwater Aquifer Layers With Schlumberger Configuration In Salma Park. Kutai Basin Geosciences, 2(2), 1–7.

Sadewo, H. H., & Djayus, D. (2024). Identification of aquifers using geoelectric mapping and sounding methods in Tanah Merah village, North Samarinda district. AIP Conference Proceedings, 3095(1), 040004. https://doi.org/10.1063/5.0204787.

Supriatna S., Sukardi R., Rustandi E. (1995). Peta Geologi Lembar Samarinda, Kalimantam Timur, Bandung: Pusat Penelitian dan Pengembangan Geologi

Suryo, D. K., Supriyanto, & Djayus. (2016). Studi Sebaran Potensi Air Tanah Di Kelurahan Tanah Merah Kecamatan Samarinda Utara Berdasarkan Resistivitas Batuan. Prosiding Seminar Sains Dan Teknologi FMIPA Unmul Periode Maret 2016, 439.

Syifaurrohman, Y., Utama, W., Lestari, W., & Surya, T. M. A. (2018). Distribusi Sebaran Akuifer Air Tanah Menggunakan Data Resistivitas Metode Vertical Electrical Sounding (VES) Konfigurasi Schlumberger (Studi Kasus Kabupaten Palu Provinsi Sulawesi Tengah). Jurnal Geosaintek, 4(3), 113. https://doi.org/10.12962/j25023659.v4i3.4102.

Syukri, M. (2020). Dasar-Dasar Metode Geolistrik (R. Safitri (ed.); 1st ed.). Syiah Kuala University Press.

Telford, W. M., Geldart, L. P., & Sheriff, R. E. (1990). Applied Geophysics (2nd ed.). Cambridge University Press.

Usman, B., Manrulu, R. H., Nurfalaq, A., & Rohayu, E. (2017). Identifikasi Akuifer Air Tanah Kota Palopo Menggunakan Metode Geolistrik Tahanan Jenis Konfigurasi Schlumberger. Jurnal Fisika FLUX, 14(2), 65. https://doi.org/10.20527/flux.v14i2.4091.